CHAPTER V
DIELECTRIC PROPERTIES AND MICROSTRUCTURE OF BARIUM STRONTIUM TITANATE (BST) CERAMICS

5.1 Abstract

Nanosized barium strontium titanate ($Ba_{1-x}Sr_xTiO_3$) particles were prepared by sol-gel method and calcined at 800 °C with varying strontium molar fraction (x = 0, 0.3, 0.5, and 0.7). The crystal structures and lattice parameters of the sol-gel $Ba_{1-x}Sr_xTiO_3$ powders and $Ba_{1-x}Sr_xTiO_3$ after sintering process at 1350 °C were investigated by XRD as a function of the strontium fraction. The $Ba_{1-x}Sr_xTiO_3$ ceramics exhibited paraelectric state at x = 0.5 and 0.7, and ferroelectric state at x = 0 and 0.3. The average grain size of $Ba_{1-x}Sr_xTiO_3$ ceramics decreased as strontium molar fraction increased. The dielectric properties of $Ba_{1-x}Sr_xTiO_3$ ceramics were measured as functions of frequency and temperature in order to observe relaxation behaviors and Curie temperature.

Keyword: Barium strontium titanate, Sol-gel method, Dielectric properties, Microstructure

5.2 Introduction

In recent year, barium strontium titanate ($Ba_{1-x}Sr_xTiO_3$) is of great interest for a material widely used in many electronic applications such as piezoelectric sensor, dynamic random access memories (DRAM), microwave phase shifter and infrared detectors because of its particular properties including high dielectric constant, low loss tangent and piezoelectric property [1-2]. The Curie temperature of pure $BaTiO_3$ exhibits dielectric peak with high dielectric constant (~10000) at Curie temperature (~130 °C) [3]. This dielectric peak can shift toward room temperature by incorporating strontium into the lattice [4, 5]. The $Ba_{1-x}Sr_xTiO_3$ (BST) is ferroelectric at room temperature for barium rich composition (x < 0.35) [6]. As strontium molar fraction increase, Curie temperature of BST shifts to lower room temperature. By this

way, BST can be a paraelectric at room temperature. Previously, many literatures have been studied the dielectric properties of BST ceramics in ferroelectric phase. However, few studies have been reported the dielectric properties in the paraelectric state. The loss tangent, which is an important factor in the electronic application, is usually lower in the paraelectric state than in the ferroelectric state. [7].

In this work, sol-gel method was selected for preparation because of particular advantages in obtaining fine powders with high chemical purity, narrow size distribution, and homogeneity through a lower temperature process, avoiding contamination of the materials. Also, it helps to maintain homogeneous mixing of two cations at molecular level [8, 9].

The objective of this study is to synthesize nano-sized BST powder using sol-gel method and investigate the effect of Sr ions substituting into Ba ions on the microstructure and dielectric properties of BST ceramics. The strontium molar fraction (x) was varied by x = 0, 0.3, 0.5 and 0.7 in order to adjust Curie temperature and obtain BST ceramics in paraelectric and ferroelectric phase at room temperature.

5.3 Experimental

5.3.1 Synthesis of Barium Strontium Titanate Nanocrystalline powders

All of the chemical used for synthesis were analytical grade, and no further purification was performed before use. For preparation of sol-gel precursor gel, barium acetate [$Ba(CH_3COO)_2$, purity > 99%, Aldrich], strontium acetate [$Sr(CH_3COO)_2$, purity > 99%, Fluka], and titanium (iv)n-butoxide [$Ti(O(CH)_3CH_3)_4$, Aldrich] were used as starting materials. Gracial acetic acid [CH_3COOH, Labscan] and methanol [CH_3OH, Labscan] were used as solvent. The barium acetate and strontium acetate were firstly dissolved in heat acetic acid with stirring to obtain clear solution followed by adding methanol with acetic acid: methanol ($R_{ac/me}$) of 1:2. The BST were prepared by varying the composition of strontium fraction with x = 0, 0.3, 0.5, and 0.7. Then the equimolar amounts of titanium (iv) n-butoxide was added into this mixture under vigorous stirring. The clear solution was stable and became a gel in a few days at room temperature. The precursor gel was converted to a dried gel by heating in vacuum oven. The dried gel was calcined by using 2-step thermal

decomposition in air at 500°C and 800°C in order to decompose the solvent and crystallize the BST (Figure 3.1).

5.3.2 Preparation of Barium Strontium Titanate Ceramic

The sol-gel BST powders with various the strontium compositions were mixed with small amount of poly (methyl methacrylate-co-ethyl acrylate) as binder and then pressed into disks shape by using a force of 10 tons for 10 mins. The sintering process was performed by putting BST disks into the furnace by using the following temperature program as shown in Figure 3.2. The temperature increases from room temperature to 300°C with heating rate of 2.1 °C/min and hold for 2 h. Then, the temperature increases to 550°C with the heating rate of 2.1 °C/min and hold for 5 h in order to remove binder out completely. Afterward, the samples were sintered at 1350 °C for 2 h with heating rate of 4.5 °C/min from 550 °C. After sintering, the specimens were cooled to room temperature at the rate of 1.7 °C/min.

5.3.3 Characterizations

The diffraction pattern of the sol-gel BST powders and BST ceramics were examined using X-ray diffraction (Rigaku, model Dmax 2002) with Cu Kα radiation and Ni-filter operated at 40 kV and 30 mA. XRD patterns were taken in the continuous mode in the 2θ range of 5-90° with the scan speed of 5 min^{-1} and sampling step of 0.02. Lattice parameters (*a* and *c*) were calculated by using the equation given below:

Cubic phase:
$$\sin^2\theta_{(hkl)} = \frac{\lambda^2(h^2+k^2+l^2)}{4a^2} \quad (5.1)$$

Tetragonal phase:
$$\sin^2\theta_{(hkl)} = \frac{\lambda^2(h^2+k^2)}{4a^2} + \frac{\lambda^2(l^2)}{4c^2} \quad (5.2)$$

The particle size of sol-gel BST powders was observed by transmission electron microscope (TEM; 100 keV, JEM-1230, JEOL). The microstructure of sintered BST (BST ceramic) was investigated by using scanning electron microscope (SEM; JSM-5200, JEOL). All specimens were coated by gold sputtering before SEM analysis. The polarization and electric field characteristics (Hysteresis loop) were measured by RT66A: standardized ferroelectric measurement test system. The specimens were immersed in silicone oil at room temperature to observed hysteresis loops.

For the sample preparation for dielectric and ferroelectric measurement, the BST ceramics were polish by SiC in order to obtain flat and parallel surfaces. The deviation in thickness affects to the experimental error in dielectric measurement. The BST ceramics were electroded by coating gold on both surfaces. The dielectric properties were measured using Hewlett-Packard 4194A impedance/gain phase analyzer. The measurements were performed by varying frequency in the range of 1 kHz – 10 MHz and temperature in the range of -60-180 °C. The dielectric constant was calculated from the capacitance by using the following equation:

$$K = \frac{CA}{\varepsilon_0 d} \tag{5.3}$$

where C is the capacitance (F), ε_0 the free space dielectric constant value (8.85×10^{-12} F/m), A the capacitor area (m^2), and d the thickness of specimens.

5.4 Results and Discussion

5.4.1 Sol-Gel Barium Strontium Titanate Powder

To observe the morphology (particle size, shape and agglomeration) of the sol-gel BST powders at various strontium molar fractions (x = 0, 0.3, 0.5, and 0.7), TEM micrographs were used to observe, as shown in Figure 5.1. The shape of all sol-gel BST powders calcined at 800 °C is irregular shape. The average size of all BST particles estimated from TEM micrographs was around 50-80 nm in diameter. The particle size and shape distribution was nearly uniform and particles are mostly agglomerated.

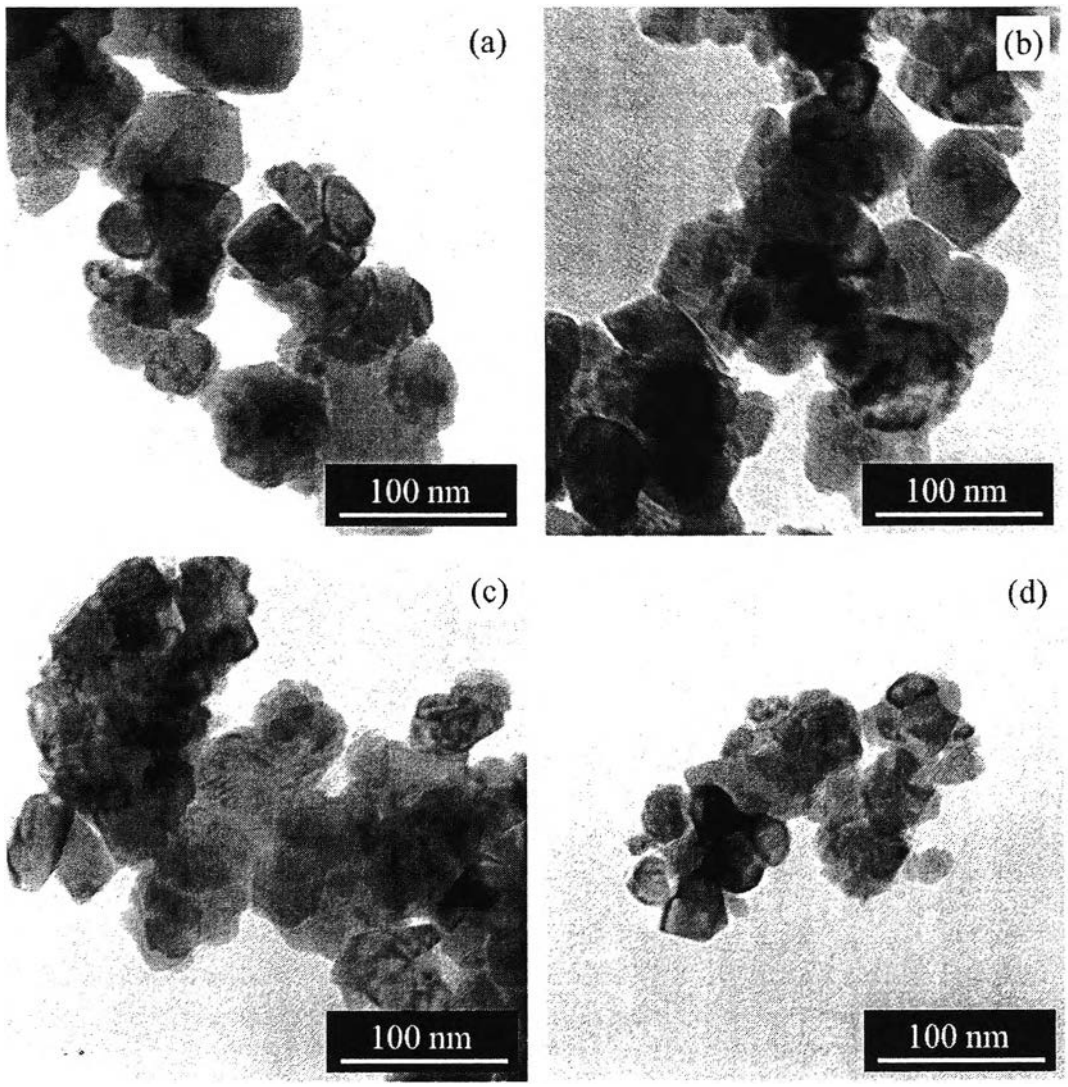

Figure 5.1 TEM micrographs of sol-gel $Ba_{1-x}Sr_xTiO_3$ powders at various strontium molar fractions (a) $x = 0$, (b) $x = 0.3$, (c) $x = 0.5$, and (d) $x = 0.7$.

5.4.2 Effect of Strontium Molar Fraction on Crystal Structure

To confirm the single phase of the sol-gel BST powders at various strontium compositions, X-ray diffraction patterns were investigated. Figure 5.2 shows XRD patterns of the sol-gel BST powders with $x = 0$, 0.3, 0.5 and 0.7, which were calcined at 800 °C. It can be seen that all diffraction patterns show perovskite structure in cubic phase. The undesirable phase ($Ba(Sr)CO_3$), a regular feature of acetic synthesis, was observed for $x = 0.5$. Beside the peak of $Ba(Sr)TiO_3$, and $Ba(Sr)CO_3$, the diffraction peaks at around $2\theta = 27°$ was also observed, which

corresponded to the intermediate oxycarbonate such as ($Ba_2Ti_2O_5CO_3$) and ($(BaSr)_2Ti_2O_5CO_3$) [10]. To suppress these undesirable phases, the calcination temperature or time should be increased in order to obtain single phase of $Ba(Sr)TiO_3$.

Moreover, it was found that the area of the diffraction peaks in XRD pattern of the sol-gel BST increased with increasing strontium fraction because of difference in reactivity between Ba^{2+} and Sr^{2+}. The Ba ions are more reactive than the Sr ions. The charge density and electronegativity of Ba^{2+} are smaller than those of Sr^{2+}, so –OR and/or –OH groups coordinated to the Ba ions in the sol solution can probably leave easier than those coordinated to the Sr ions. From this reason, it indicated that the gel formation had higher degree of crystallization at higher barium concentration [11].

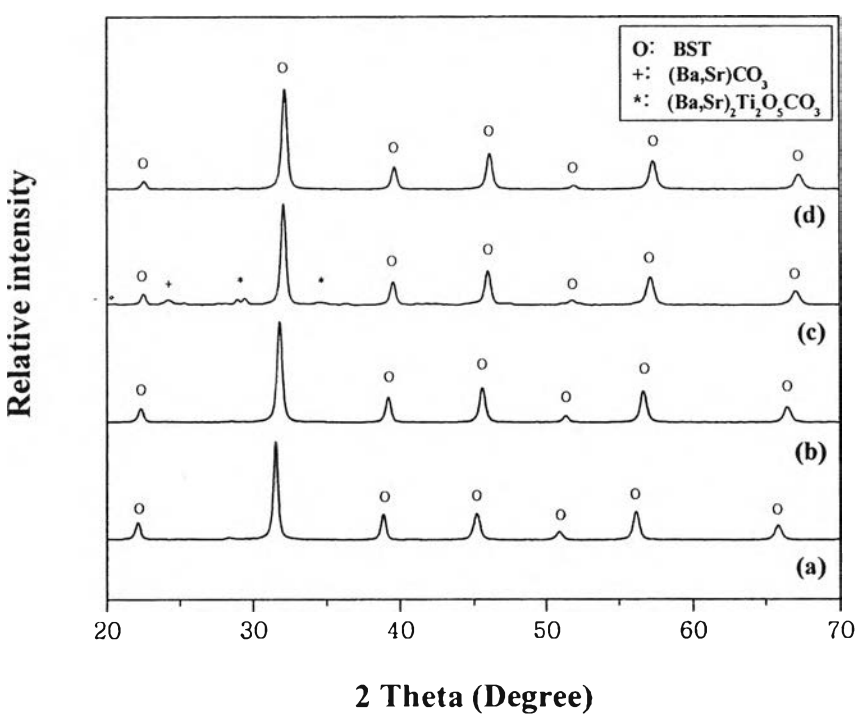

Figure 5.2 XRD patterns of sol-gel $Ba_{1-x}Sr_xTiO_3$ powders calcined at 800 °C for 80 min: (a) x = 0, (b) x = 0.3, (c) x = 0.5, (d) x = 0.7 (Note: ○ = BST, + = $Ba(Sr)CO_3$, and * = $(Ba,Sr)_2Ti_2O_5CO_3$).

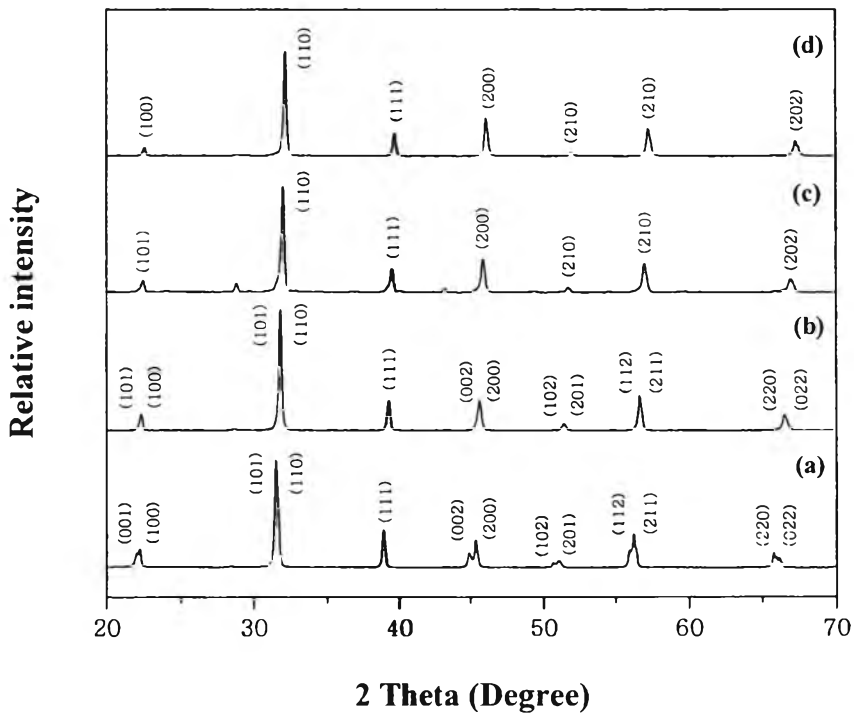

Figure 5.3 XRD patterns of $Ba_{1-x}Sr_xTiO_3$ ceramics sintered at 1350 °C for 2 h: (a) x = 0, (b) x = 0.3, (c) x = 0.5, (d) x = 0.7.

All characteristic peaks of the sol-gel BST powders show cubic structure. After sintering process, the structure of BST ceramics with the strontium molar fraction of x = 0 and 0.3 changed from cubic to tetragonal, which can be indicated by the splitting of the diffraction peak at $2\theta \approx 45°$ [(002)/(200)] [12, 13]. When the strontium fraction (x) was greater than 0.3, the BST ceramics were cubic structure. The shift of the diffraction peaks to higher 2θ with increasing strontium fractions can be observed in Figure 5.2 and Figure 5.3, which indicated that the lattice parameter became small with increasing strontium fraction. The reduction of lattice parameters was caused by the substitution of the smaller ionic radius Sr^{2+} (1.40 Å) into the Ba^{2+} (1.60 Å) in the lattice [14].

The lattice parameter of the sol-gel BST powders compared with the BST ceramics as a function of the strontium fraction (x) is shown in Figure 5.4. It can be seen that the lattice parameters of the sol-gel BST powders were larger than that of BST ceramics. This result may be explained by the effect of remaining OR or

OH group in the structure of sol-gel BST powders [11]. The lattice parameters (*a* and *c*) and tetragonality (*c*/*a*) of the sol-gel BST powders and BST ceramics at different strontium molar fractions are summarized in Table 5.1 and Table 5.2, respectively.

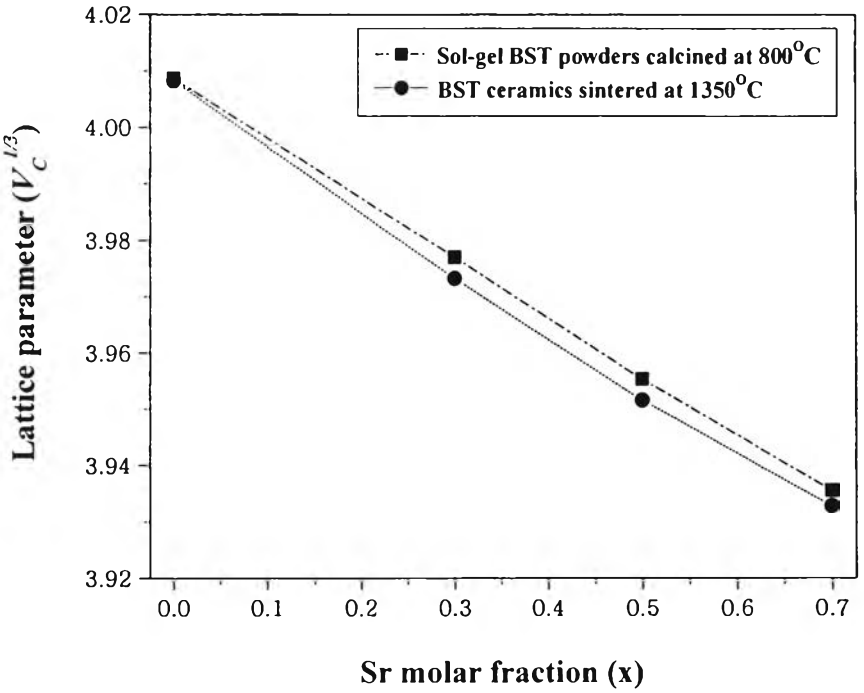

Figure 5.4 Average lattice parameter ($V_c^{1/3}$) of $Ba_{1-x}Sr_xTiO_3$ ceramics sintered at 1350 °C at various strontium molar fractions (x = 0, 0.3, 0.5, and 0.7).

Table 5.1 Lattice parameters, tetragonality and structure of sol-gel $Ba_{1-x}Sr_xTiO_3$ powders

Strontium Molar Fraction (x)	Lattice parameter (Å)		Volume of unit cell (Å^3)	Tetragonality (c/a)	Structure
	a	c			
0	4.0087	4.0087	64.42	1	Cubic
0.3	3.9772	3.9772	62.91	1	Cubic
0.5	3.9555	3.9555	61.89	1	Cubic
0.7	3.9357	3.9357	60.96	1	Cubic

Table 5.2 Lattice parameters, tetragonality and structure of $Ba_{1-x}Sr_xTiO_3$ ceramics

Strontium Molar Fraction (x)	Lattice parameter (Å)		Volume of unit cell (Å^3)	Tetragonality (c/a)	Structure
	a	c			
0	3.9967	4.0315	64.40	1.0087	Tetragonal
0.3	3.9728	3.9745	62.73	1.0004	Tetragonal
0.5	3.9517	3.9517	61.71	1	Cubic
0.7	3.9330	3.9330	60.84	1	Cubic

5.4.3 Microstructure of Barium Strontium Titanate Ceramics

The microstructures of the BST ceramics after sintering at 1350 °C for 2 h with strontium fraction of x = 0, 0.3, 0.5, and 0.7 are shown by SEM micrographs in Figure 5.5. It can be obviously seen that the average grain size of BST ceramics ranged from 11 to 3 μm and decreased with increasing strontium molar fraction. This was argued that the ceramic and liquid phase became more refractory as strontium content increased [15]. The average grain size of BST ceramic at all strontium compositions are also listed in Table 5.3.

Table 5.3 Average grain size of $Ba_{1-x}Sr_xTiO_3$ ceramics at various strontium molar fractions (x)

Strontium Molar Fraction (x)	Average grain size (μm)
0	10.82
0.3	7.99
0.5	3.88
0.7	2.91

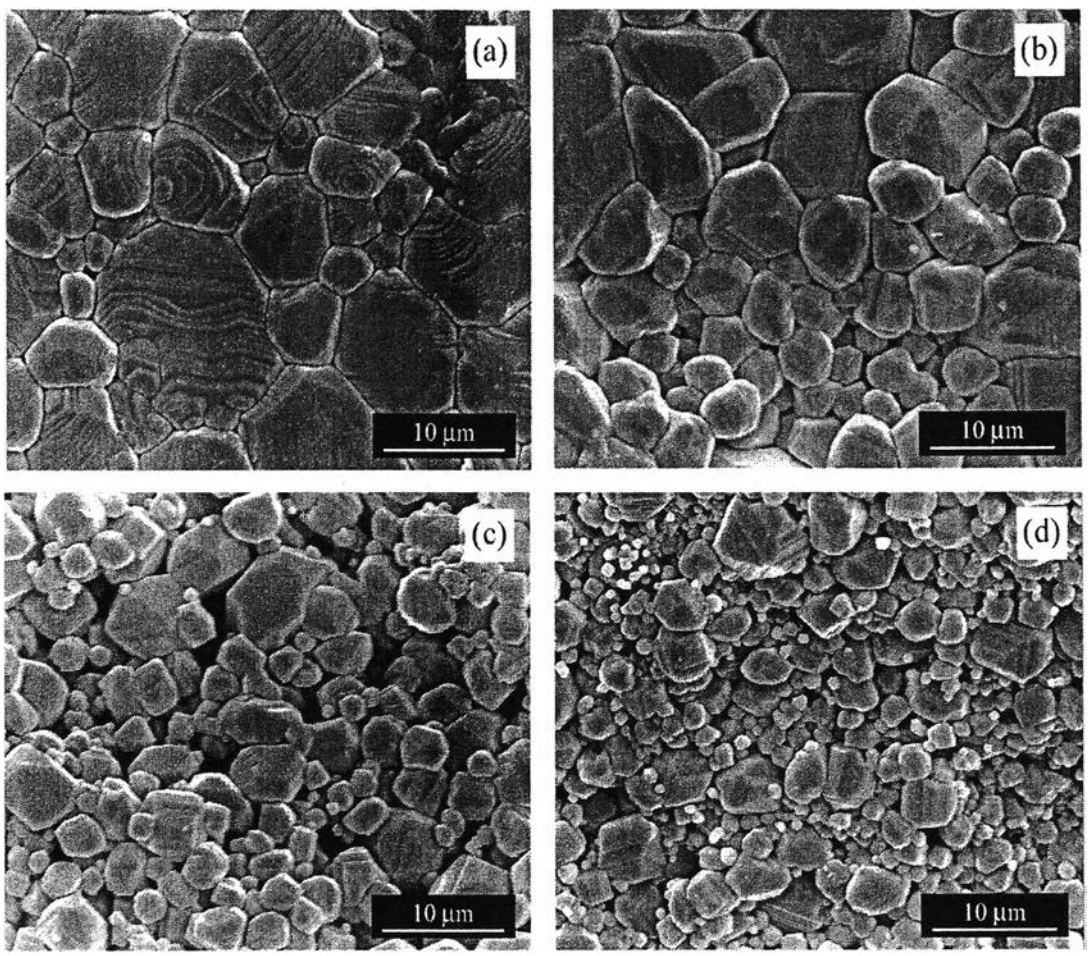

Figure 5.5 SEM micrographs of $Ba_{1-x}Sr_xTiO_3$ ceramics: (a) $x = 0$. (b) $x = 0.3$, (c) $x = 0.5$, (d) $x = 0.7$ (sintering at 1350 °C, 2 h).

5.4.4 Ferroelectric Measurement

The ferroelectric and paraelectric behavior of the BST ceramics were investigated from relationship between polarization (P) and electric field (E) at room temperature, as shown in Figure 5.6. It was found that the hysteresis loop of BST ceramics with $x = 0$ and 0.3 can be observed, which shows characteristic of ferroelectric. For the strontium fraction of 0.5, it shows linearly relation of polarization and electric field indicating the paraelectric.

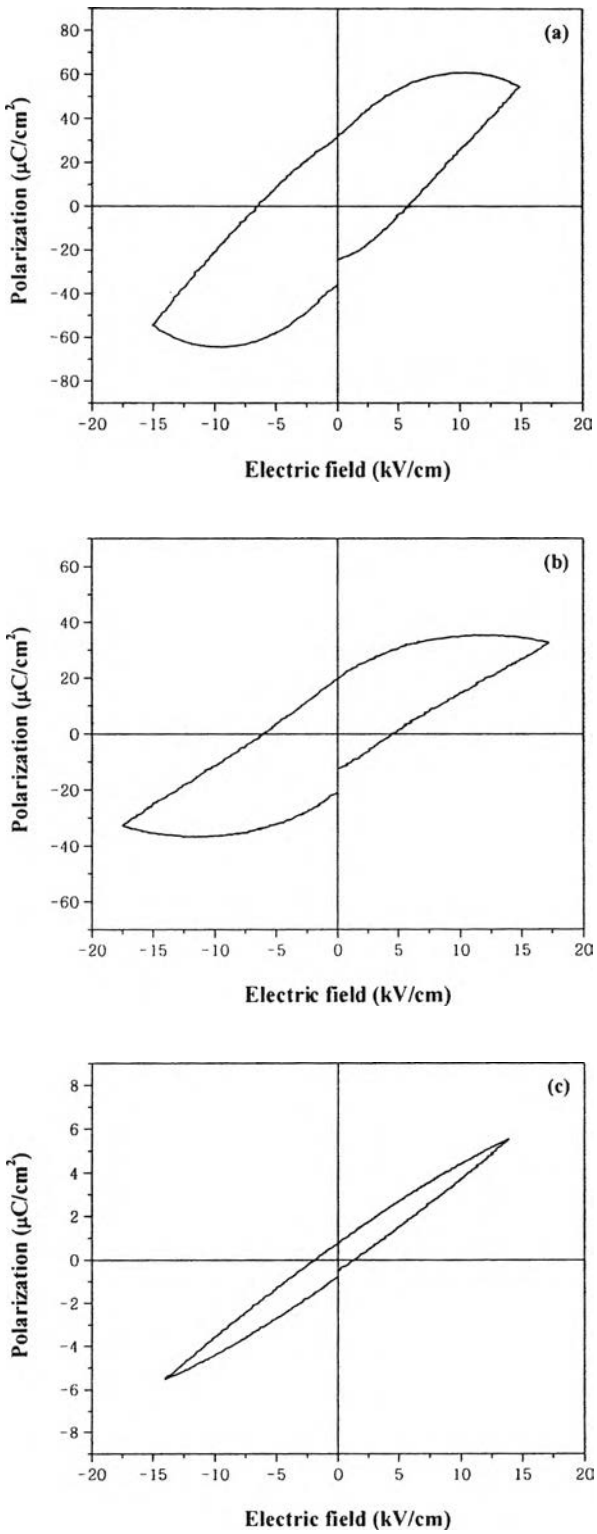

Figure 5.6 Hysteresis loop of $Ba_{1-x}Sr_xTiO_3$ ceramics at room temperature: (a) $x = 0$, (b) $x = 0.3$, and (c) $x = 0.5$.

5.4.5 Dielectric Properties of Barium Strontium Titanate Ceramics

5.4.5.1 Frequency Dependence of Dielectric Properties

The dielectric properties of the BST ceramics with various strontium fractions measured as a function of frequency range of 100 Hz -10 MHz are shown in Figure 5.7 and Figure 5.8. It shows that the highest dielectric constant (~2900) was obtained by doping strontium fraction of 0.3 because the Curie point probably shifted to near room temperature. However, their dielectric constant values dropped rapidly at high frequency (> 1 MHz) and loss tangent increased abruptly. This phenomenon was due to dipolar relaxation [7]. The dielectric constants of the BST ceramics with x = 0.5 and 0.7 were lower than those with x = 0 and 0.3, but they were low dipolar relaxation at high frequency. The loss tangent of the BST ceramics in the paraelectric phase (x = 0.5 and 0.7) were less than those in the ferroelectric phase (x = 0 and 0.3).

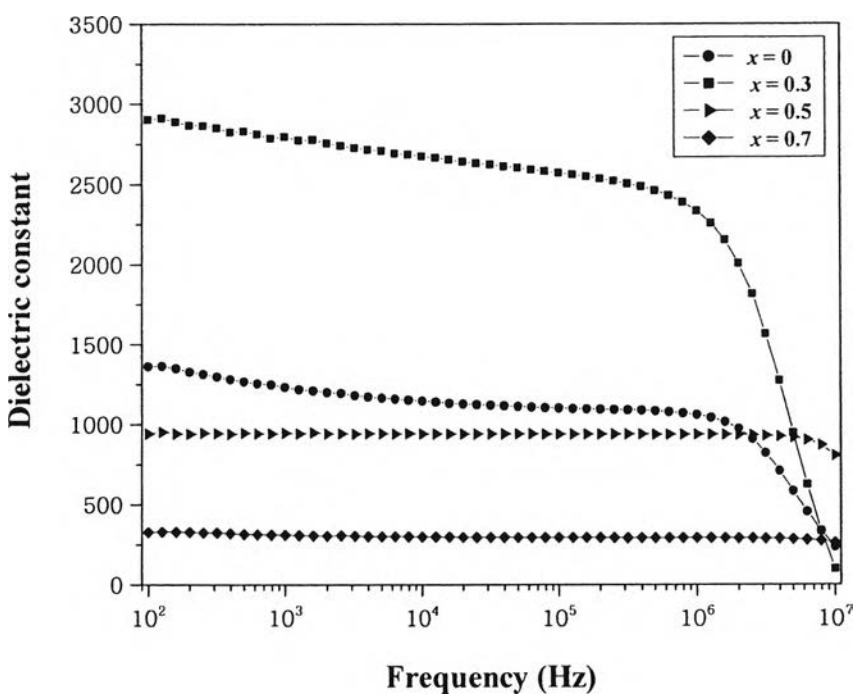

Figure 5.7 Dielectric constant of $Ba_{1-x}Sr_xTiO_3$ ceramics as function of frequency at room temperature.

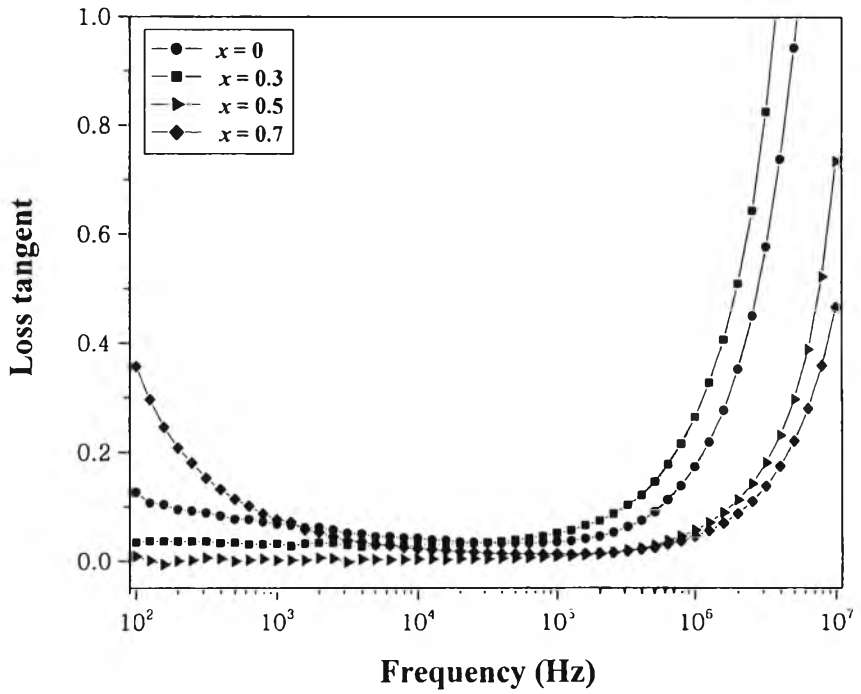

Figure 5.8 Loss tangent of $Ba_{1-x}Sr_xTiO_3$ ceramics as function of frequency at room temperature.

5.4.5.2 Temperature Dependence of Dielectric Properties

Figure 5.9-5.11 shows the dielectric constant of BST ceramics (x = 0.1, 0.3, and 0.5) versus temperature at various frequencies. The dielectric peak indicates Curie temperature (T_C) or the phase transition of ferroelectric-paraelectric. It can be seen that the dielectric peak of these ceramics was independent on changing frequency.

Figure 5.12 shows dielectric constant versus temperature in the range of -60-180 °C for various strontium compositions (x = 0.1, 0.3, 0.5 and 0.7) at 100 kHz. Zhou *et al.* reported that Curie temperature (T_C) decreased with shifting rate of 3.3 °C.mol%$^{-1}$ of strontium [14]. In the current study, it was found that T_C shifted to lower temperature with the shifting rate of 3.1 °C.mol%$^{-1}$ of strontium. T_C of pure $BaTiO_3$ was 125 °C, which was close to value from literatures. Deb *et al.* reported that T_C of pure $BaTiO_3$ was 128 °C [16]. Deshpande *et al.* prepared sol-gel derived $BaTiO_3$ ceramic and found that Curie temperature was 127 °C [8]. T_C shifted toward near room temperature (~40 °C) for x = 0.3, which indicateed that the BST

ceramic was ferroelectric phase at room temperature. The BST ceramic changes to paraelectric phase at $x = 0.5$ because T_C was below room temperature (~-35 °C). This result agrees with previous reports. Fu *et al.* reported that T_C of BST was -30 °C [6]. These results correspond to XRD and hysteresis study (5.4.2 and 5.4.3). For T_C of the BST ceramic with $x = 0.7$, it could not be observed dielectric peak because operating temperature of instrument limit at -60 °C. From these results, it was concluded that T_C decreased with increasing strontium molar fraction (x) as a linear relation, as shown in Figure 5.13. T_C of the BST ceramics with all strontium compositions are listed in Table 5.4.

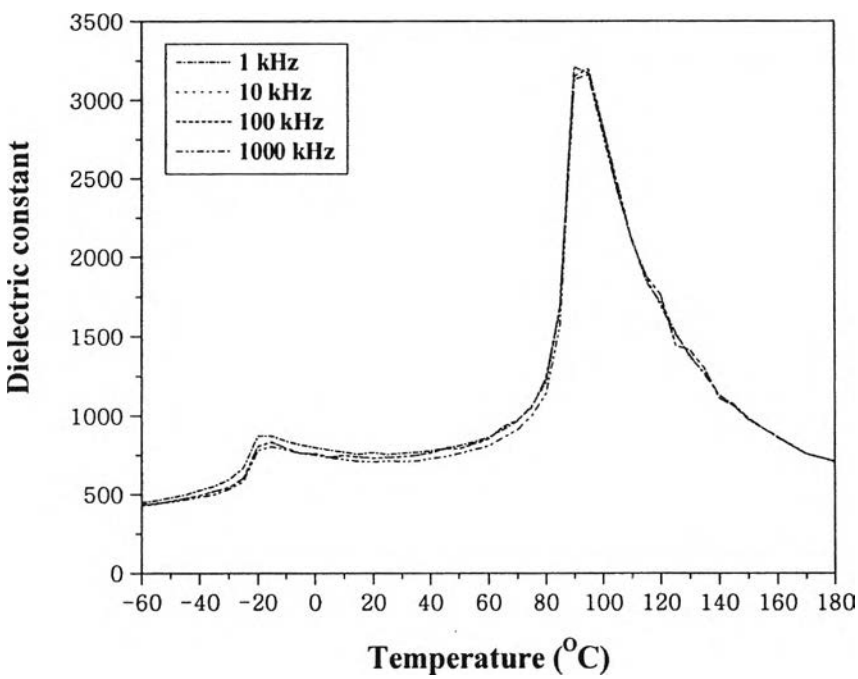

Figure 5.9 Temperature dependence of dielectric constant at various frequencies for $Ba_{0.9}Sr_{0.1}TiO_3$ ceramic.

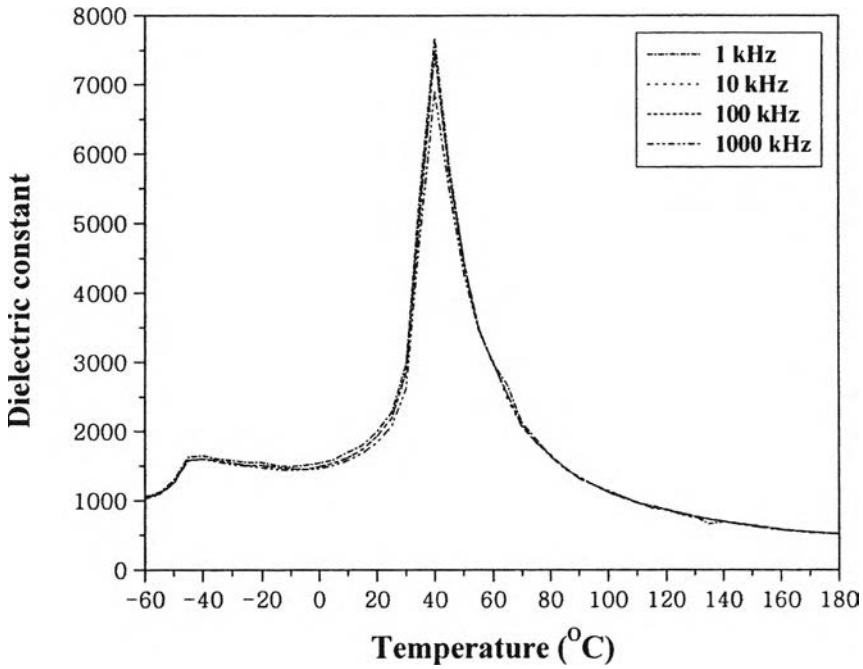

Figure 5.10 Temperature dependence of dielectric constant at various frequencies for $Ba_{0.7}Sr_{0.3}TiO_3$ ceramic.

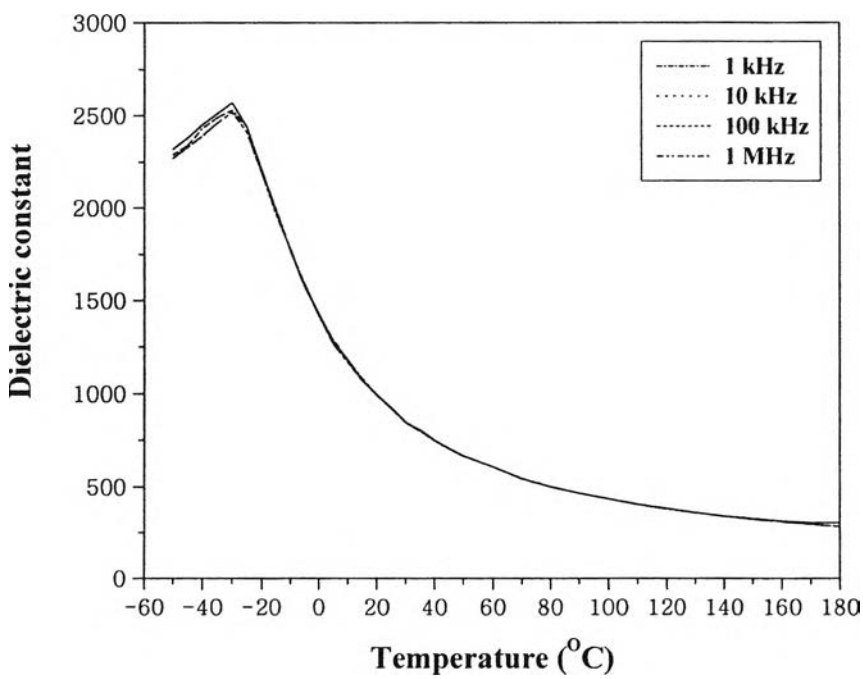

Figure 5.11 Temperature dependence of dielectric constant at various frequencies for $Ba_{0.5}Sr_{0.5}TiO_3$ ceramic.

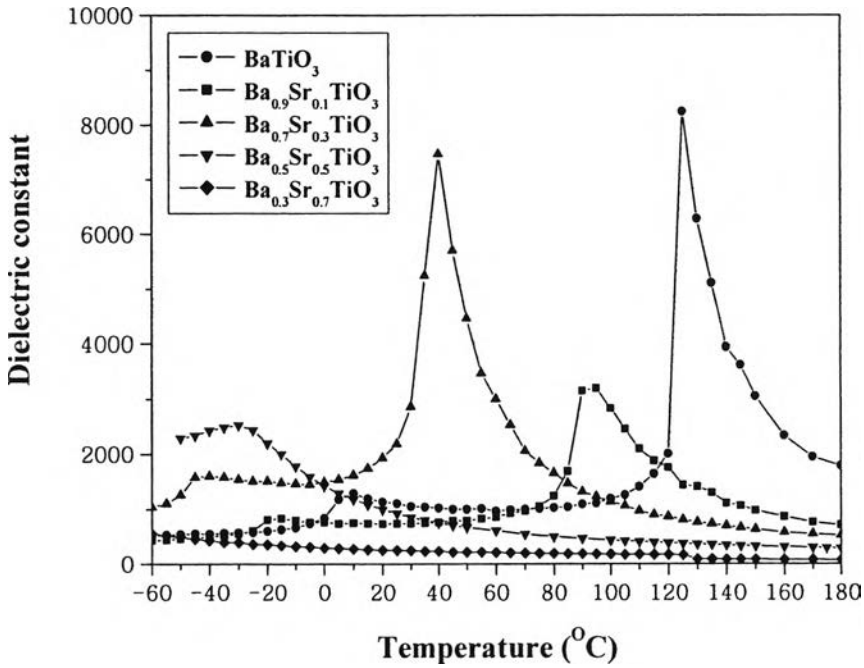

Figure 5.12 Dielectric constant as a function of temperature for $Ba_{1-x}Sr_xTiO_3$ (x = 0, 0.1, 0.3, 0.5 and 0.7) ceramics at 100 kHz.

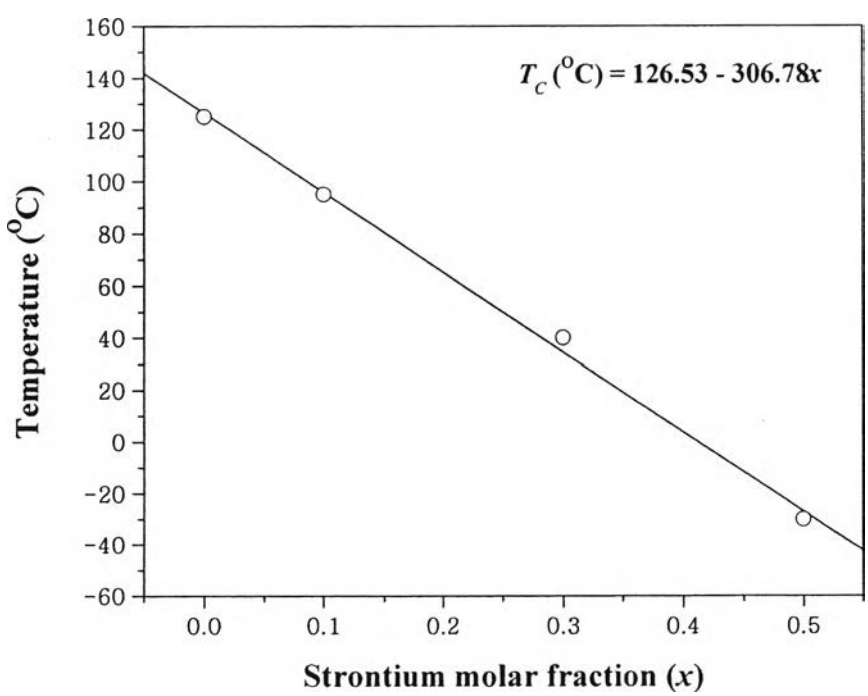

Figure 5.13 Relationship between Curie temperature and strontium molar fraction.

Table 5.4 Structure, phase, and Curie temperature of $Ba_{1-x}Sr_xTiO_3$ ceramics at various strontium molar fractions (x)

Strontium molar fraction (x)	Structure	Phase	Curie temperature T_C (°C)
0	Tetragonal	Ferroelectric	125
0.1	Tetragonal	Ferroelectric	95
0.3	Tetragonal	Ferroelectric	40
0.5	Cubic	Paraelectric	-30
0.7	Cubic	Paraelectric	<-60

5.5 Conclusions

Fine BST nano-particle with an average size around 50-80 nm were successfully synthesized by sol-gel method. The structure of the sol-gel powders at all compositions were cubic phase. After sintering, BST ceramics at x = 0 and 0.3 changed to tetragonal structure and existed cubic structure for x = 0.5 and 0.7. The lattice parameters of BST decreased with increasing the strontium molar fraction. This is due to the Sr^{2+} ionic radius smaller than that of Ba^{2+}. The average grain size of BST ceramics decreased from 11 μm for x = 0 to 3 μm for x = 0.7 as strontium molar fraction increased. Hysteresis loop measurement showed the characteristic of the paraelectric phase for x = 0.5 and the ferroelectric phase for x = 0 and 0.3. For dielectric measurement, the dielectric constant of the $Ba_{0.7}Sr_{0.3}TiO_3$ (x = 0.3) showed the highest value comparing with other compositions, and dipolar relaxation was observed at frequencies above 1 MHz. While the BST ceramics with x = 0.5 and 0.7 had low relaxation and loss tangent. T_C linearly decreased with increasing the amount of strontium. By doping strontium molar fraction of 0.5, T_C decreased from 125°C for pure $BaTiO_3$ to -30°C.

5.6 Acknowledgements

The authors wish to thank Dr. Pitak Laoratanakul and MTEC staffs for useful assistance and instrument for characterizations. Also, it was achieved thanks to research grants from the Government Research Budget Year 2005-2006 Petroleum and Petrochemical College; the National Excellence Center for Petroleum, Petrochemical , and Advanced Materials, Thailand.

5.7 References

[1] G.W. Dietz, M. Shumacher, R. Waser, S.K. Streiffer, C. Basceri, and A.I. Kingon, "Leakage current in $Ba_{0.7}Sr_{0.3}TiO_3$ thin film for ultrahigh density dynamic random access memories," *Journal of Applied Physics*, vol. 82(5), pp. 2359-2364, 1997.

[2] T.N. Lin, J.P. Chu, and S.F. Wang, "Structure and properties of $Ba_{0.3}Sr_{0.7}TiO_3$:$MgTiO_3$," *Materials Letters*, vol. 59, pp. 2786-2789, 2005.

[3] R. Ganesh and E. Goo, "Microstructure and dielectric characteristic of $(Pb_xBa_{0.5-x}Sr_{0.5})TiO_3$," *Journal of the American Ceramic Society*, vol. 79(1), pp. 225-232, 1996.

[4] M. Klee, "Low-temperature processing of $BaTiO_3$, $BaTi_{1-x}Zr_xO_3$ and $Ba_{1-x}Sr_x$ TiO_3 powder," *Journal of Material Science Letters*, vol. 8(8), pp. 985-988, 1989.

[5] N.V. Giridharan, R. Varatharajan, R. Jayavel, and P. Ramasamy, "Fabrication and characterization of $(Ba,Sr)TiO_3$ thin film by sol-gel technique through organic precursor route," *Materials Chemistry and Physics*, vol. 65, pp. 261-265, 2000.

[6] C. Fu, C. Yang, H. Chen, Y. Wang, and L. Hu, "Microstructure and dielectric properties of $Ba_xSr_{1-x}TiO_3$ ceramics," *Materials Science and Engineering B*, vol. 119, pp. 185-188, 2005.

[7] J.W. Liou and B.S. Chiou, "Dielectric characteristic of doped $Ba_{1-x}Sr_xTiO_3$ at the paraelectric state," *Materials Chemistry and Physics*, vol. 51, pp. 59-63, 1997.

[8] S.B. Deshpande, P.D. Godbole, Y.B. Khollam, and H.S. Potdar, "Characterization of barium titanate: $BaTiO_3$ (BT) ceramics prepared from sol-gel derived BT powders," *Journal of Electroceramics*, vol 15, pp. 103-108, 2005.

[9] W. Yang, A. Chang, and B. Yang, "Preparation of barium strontium titanate ceramic by sol-gel method and microwave sintering," *Journal of Materials Synthesis and Processing*, vol. 10 (6), pp. 303-309, 2003.

[10] C. Mao, X. Dong, and T. Zeng, "Synthesis and characterization of nano-crystalline barium strontium titanate," *Materials Letters*, vol. 61(8-9), 1633-1636, 2007.

[11] H. Shibashi, H. Matsuda, and M. Kuwabara, "Low-temperature preparation of (Ba,Sr)TiO_3 perovskite phase by sol-gel method," *Journal of Sol-Gel Science Technology*, vol. 16, pp. 129-134, 1999.

[12] R.N. Viswanath and S. Ramasamy, "Preparation and ferroelectric phase transition studies of nanocrystalline $BaTiO_3$," *Nano Stuctured Materials*, vol. 8(2), pp. 155-162, 1997.

[13] T. Yan, Z.G. Shen, W.W. Zhang, and J.F. Chen, "Size dependence on the ferroelectric transition of nanosized $BaTiO_3$ particles," *Materials Chemistry and Physics*, vol. 98, pp. 450-455, 2006.

[14] L. Zhou, P.M. Vilarinho, and J.L. Baptista, "Dependence of the structure and dielectric properties of $Ba_{1-x}Sr_xTiO_3$ ceramics solid solution on raw material processing," *Journal of the European Ceramic Society*, vol. 19, pp. 2015-2020, 1999.

[15] J.W. Liou and B.S. Chiou, "Effect of direct-current on the dielectric properties of barium strontium titanate," *Journal of the American Ceramic Society*, vol. 80(12), pp. 3093-3099, 1997.

[16] K.K. Deb, M.D. Hill and J.F. Kelly, "Pyroelectric characteristics of modified barium titanate ceramics," *Journal of Materials Research*, vol. 7(12), pp. 3296-3305. 1992.